# Selenium Analogs of Tetrathiapentalene Derivatives with Long Alkyl Chains

**Masanobu Aragaki, Shinya Kimura, Mao Katsuhara, Hiroyuki Kurai, and Takehiko Mori***

Department of Organic and Polymeric Materials, Graduate School of Science and Engineering, Tokyo Institute of Technology, Meguro-ku, Tokyo 152-8552

(Received November 21, 2000)

A novel selenium-containing bis-fused tetrathiafulvalene donor, $C_2$TET-TS-TTP (2-[4,5-bis(ethylthio)-1,3-dithiol-2-ylidene]-5-(4,5-ethylenedithio-1,3-diselenol-2-ylidene)-1,3,4,6-tetrathiapentalene), has been synthesized. The $ClO_4^-$, $BF_4^-$, and $PF_6^-$ salts of $C_2$TET-TS-TTP are isostructural, having uniform $\beta$-type structures. These salts are essentially metallic down to low temperatures.

Bis-fused TTF derivatives, which are usually called TTP (tetrathiapentalene) donors, are excellent organic donors. They form highly conducting radical-cation salts with a variety of anions, because these donors construct a two-dimensional network for electrical conduction. Although many salts are metallic down to low temperatures, they do not show superconductivity except for $(DTEDT)_3[Au(CN)_2]$.[1–3] Recently, new TTP derivatives with long alkyl chains, $C_n$TET-TTP, have been synthesized.[4] Among them, $C_2$TET-TTP (2-[4,5-bis(ethylthio)-1,3-dithiol-2-ylidene]-5-(4,5-ethylenedithio-1,3-dithiol-2-ylidene)-1,3,4,6-tetrathiapentalene), Scheme 1, forms radical-cation salts with $ClO_4^-$ and $BF_4^-$; such $\beta$-type salts are metallic down to helium temperatures, although $C_1$TET-TTP (= TMET-TTP, (2-[4,5-bis(methylthio)-1,3-dithiol-2-ylidene]-5-(4,5-ethylenedithio-1,3-dithiol-2-ylidene)-1,3,4,6-tetrathiapentalene) forms $\theta$-type salts regardless of the counter anions and these salts are semiconductive below 200 K. This study suggests that the replacement of the methylthio groups by the ethylthio groups is an effective strategy to change the donor arrangement and to stabilize the metallic states.

On the other hand, replacement of sulfur atoms of TTP skeleton with other chalcogen atoms, such as selenium, has been carried out as an attractive modification, because of the strengthened transverse chalcogen–chalcogen interaction due to larger electron clouds of selenium atoms and the resultant stabilization of a low-temperature metallic state. Furthermore, the partial selenium substitution seems to increase the possibility that we can get crystals suitable for structure analysis.

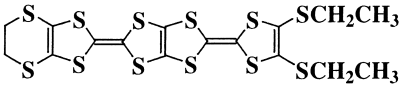


$C_2$TET-TTP

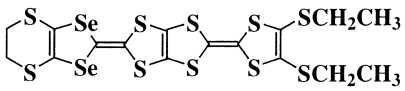


$C_2$TET-TS-TTP **1**

Scheme 1.

Since the synthesis of the first selenium analog of TTP, 2-(1,3-diselenol-2-ylidene)-5-(1,3-dithiol-2-ylidene)-1,3,4,6-tetrathiapentalene (ST-TTP),[5] various modifications of this strategy for other TTP derivatives have been attempted. In this article we describe syntheses, structures and physical properties of charge transfer salts of a selenium analog of $C_2$TET-TTP, in which two sulfur atoms of the terminal 1,3-dithiole ring of the ET side are replaced by selenium atoms. Following Misaki's notation, this molecule (**1** in scheme 1) will be hereafter called $C_2$TET-TS-TTP.

## Results

**Preparation.** The synthesis of $C_2$TET-TS-TTP (**1**) was achieved following the reported method, as shown in Scheme 2.[5,6] The trimethyl phosphite-mediated cross-coupling reaction between **3** and 4,5-ethylenedithio-1,3-diselenol-2-one (**4**)[7] in refluxing toluene afforded $C_2$TET-TS-TTP (17%).

**Electrochemical Properties.** The solution redox properties of $C_2$TET-TS-TTP and $C_2$TET-TTP have been studied by cyclic voltammetry. The results are listed in Table 1. These donors show four reversible redox couples up to 4+, which correspond to the oxidation of the four 1,3-chalcogenole rings. The first redox potential of $C_2$TET-TS-TTP is a little higher (0.05 V) than that of $C_2$TET-TTP. The $E_2-E_1$ value of $C_2$TET-TS-TTP, which corresponds to the on-site Coulomb repulsion, was smaller by 0.01 V than that of $C_2$TET-TTP.

**Crystal Structures.** Crystals were grown by electrochemical oxidation in chlorobenzene in the presence of the donor and a tetrabutylammonium salt of the corresponding anions under a constant current of 0.2 μA at 26 °C using H-shaped cells with Pt electrodes. In the presence of $ClO_4^-$, $BF_4^-$, $PF_6^-$, $I_3^-$, and $[Au(CN)_2]^-$ single crystals in the form of black needles were obtained (Table 2).

X-ray single crystal structure analysis was carried out for $(C_2$TET-TS-TTP$)_2ClO_4$, $(C_2$TET-TS-TTP$)_2BF_4$, and $(C_2$TET-TS-TTP$)_2PF_6$ (Table 3).

The lattice constants of $(C_2$TET-TS-TTP$)_2ClO_4$ are almost the same as those of $(C_2$TET-TTP$)_2ClO_4$ (shown in the bottom of Table 3),[4] indicating that these salts are isostructural. All

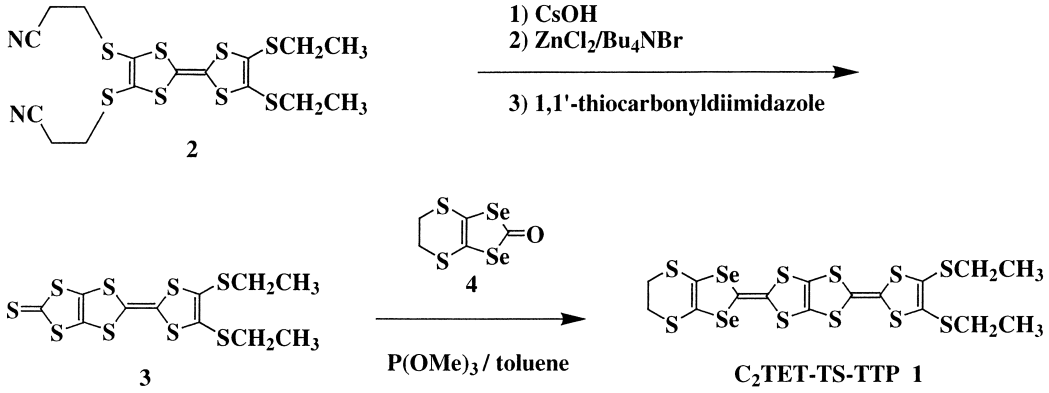


Scheme 2. Synthesis of $C_2$TET-TS-TTP.

Table 1. Electrical Redox Potentials (V) vs. Ag/AgCl in $(n\text{-Bu})_4NPF_6$/Benzonitrile at a Pt Working Electrode

| Compound | $E_1$ | $E_2$ | $E_3$ | $E_4$ | $E_2-E_1$ |
|---|---|---|---|---|---|
| $C_2$TET-TTP | +0.44 | +0.68 | +0.94 | +1.18 | +0.24 |
| $C_2$TET-TS-TTP | +0.49 | +0.72 | +1.00 | +1.13 | +0.23 |

Table 2. Electrical Properties of Cation Radical Salts on $(C_2TET\text{-}TS\text{-}TTP)(A)_x$

| Anion | Solvent | Form[a)] | x[b)] | $\sigma_{rt}$/S cm$^{-1}$ | Conducting behavior |
|---|---|---|---|---|---|
| $ClO_4$ | PhCl | P | 0.50(X) | 55 | Metallic down to 1.5 K |
| $BF_4$ | PhCl | P | 0.50(X) | 12 | Metallic down to 1.5 K |
| $PF_6$ | PhCl | P | 0.50(X) | 34 | Metallic down to 1.5 K |
| $I_3$ | PhCl | P | 0.9(I) | $2.3\times10^{-4}$ | $E_a$ = 0.086 eV |
| $Au(CN)_2$ | PhCl | P | 0.5(Au) | 9.2 | $E_a$ = 0.025 eV |

a) P = plates. b) Determined by the EDS from the ratio of sulfur and the elements designated in the parentheses. X presents the value determined from the single crystal X-ray structure analysis.

Table 3. Crystallographic data of $(C_2TET\text{-}TS\text{-}TTP)_2X$ (X = $ClO_4^-$, $BF_4^-$, and $PF_6^-$)

| Compound | $(C_2TET\text{-}TS\text{-}TTP)_2ClO_4$ | $(C_2TET\text{-}TS\text{-}TTP)_2BF_4$ | $(C_2TET\text{-}TS\text{-}TTP)_2PF_6$ |
|---|---|---|---|
| Molecular Formula | $C_{32}H_{28}S_{20}Se_4ClO_4$ | $C_{32}H_{28}S_{20}Se_4BF_4$ | $C_{32}H_{28}S_{20}Se_4PF_6$ |
| Formula Weight | 1469.06 | 1456.54 | 1514.70 |
| Crystal System | monoclinic | monoclinic | monoclinic |
| Space Group | *C*2/*c* | *C*2/*c* | *C*2/*c* |
| *a*/Å | 25.687(9) | 25.639(4) | 25.776(7) |
| *b*/Å | 5.920(2) | 5.910(1) | 5.939(2) |
| *c*/Å | 32.69(2) | 32.507(6) | 32.897(8) |
| $\alpha$/° | 90 | 90 | 90 |
| $\beta$/° | 96.79(3) | 96.71(1) | 96.839(4) |
| $\gamma$/° | 90 | 90 | 90 |
| *V*/Å$^3$ | 4936(3) | 4892(1) | 5001(2) |
| *Z* | 4 | 4 | 4 |
| $D_c$/g cm$^{-3}$ | 1.977 | 1.978 | 2.012 |
| $\mu$(Mo $K\alpha$)/cm$^{-1}$ | 38.49 | 38.35 | 37.91 |
| *R* | 0.066 | 0.084 | 0.051 |
| $R_w$ | 0.076 | 0.122 | 0.058 |
| Reflections measured | 7951 | 7909 | 8089 |
| Reflections used | 2581 | 1737 | 1731 |

Crystal data of $(C_2TET\text{-}TTP)_2ClO_4$: *C*2/*c*, *a* = 25.31(5), *b* = 5.842(4), *c* = 32.67(6) Å, $\beta$ = 97.94°(9), and *V* = 4784(1) Å$^3$.[4b]

lattice constants of the Se compounds are larger than those of the S compound, but the expansion is anisotropic; the increase is particularly large in the interchain direction (the *a* axis).

The atomic numbering scheme of the donor is shown in Fig.

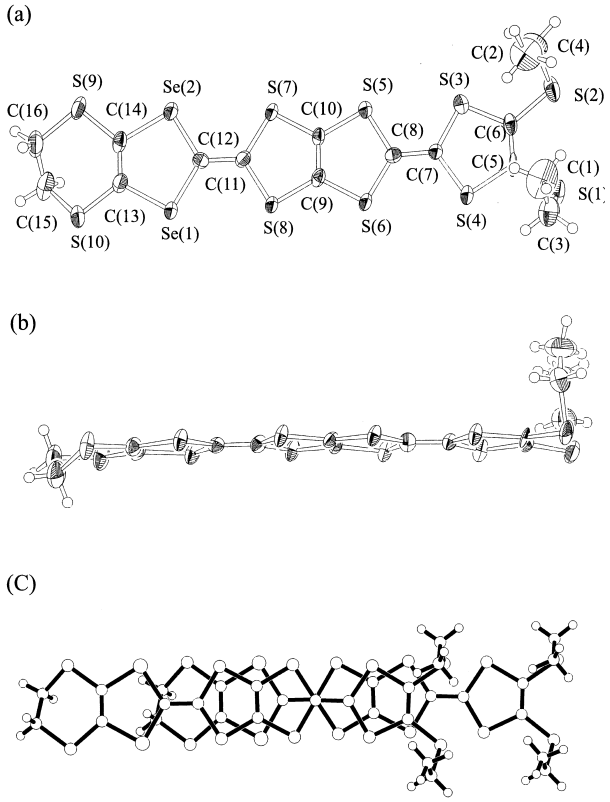


Fig. 1. (a) ORTEP drawing and atomic numbering scheme and (b) side view of the donor molecule of $(C_2TET\text{-}TS\text{-}TTP)_2ClO_4$. (c) Overlap mode of $(C_2TET\text{-}TS\text{-}TTP)_2ClO_4$.

1(a). As shown in Fig. 1(b), the TTP part of $(C_2TET\text{-}TS\text{-}TTP)_2ClO_4$ is almost flat, and the ethylthio chains extend nearly perpendicular to the TTP skeleton. Figure 2 shows the crystal structure of $(C_2TET\text{-}TS\text{-}TTP)_2ClO_4$. Similarly to $(C_2TET\text{-}TTP)_2ClO_4$, one crystallographically independent donor molecule is located on a general position and one $ClO_4^-$ anion on a two-fold axis. Thus, the ratio of donor and anion is 2:1. The donors form conducting sheets along the ab plane, as shown in Fig. 3; such sheets are separated by insulating anion layers. The arrangement of the donors is $\beta$-type. In the present $C_2TET\text{-}TS\text{-}TTP$ salts, the replacement of sulfur atoms with selenium atoms does not change the donor arrangement. This contrasts with BEDT-TTF (bis(ethylenedithio)tetrathiafulvalene) salts, where the selenium analog, BETS (bis(ethylenedithio)tetraselenafulvalene), has usually entirely different donor packings. For example, BETS affords $\kappa$- and $\lambda$-type salts with tetrahedral anions such as $GaCl_4^-$ and $FeCl_4^-$,[8] whereas the corresponding BEDT-TTF salts are $\delta'$-type.[9] This is, however, not surprising because ST-TTP, in which two of the eight sulfur atoms of TTP are replaced by selenium, affords $\beta$-type salts similarly to the original TTP.[5]

The donors form a uniform chain along the $b$ axis; all interactions in a chain, which are designated as $b$ in Fig. 3, are equivalent. In this chain the donors are stacked in a head-to-head manner (Fig. 1(c)). The overlap mode is the so-called ring-over-bond type; the interplanar distance in a stack is 3.47 Å (3.51 Å for $(C_2TET\text{-}TTP)_2ClO_4$),[4] and the slip distance along the donor long axis is 4.72 Å (4.71 Å for $(C_2TET\text{-}TTP)_2ClO_4$).[4]

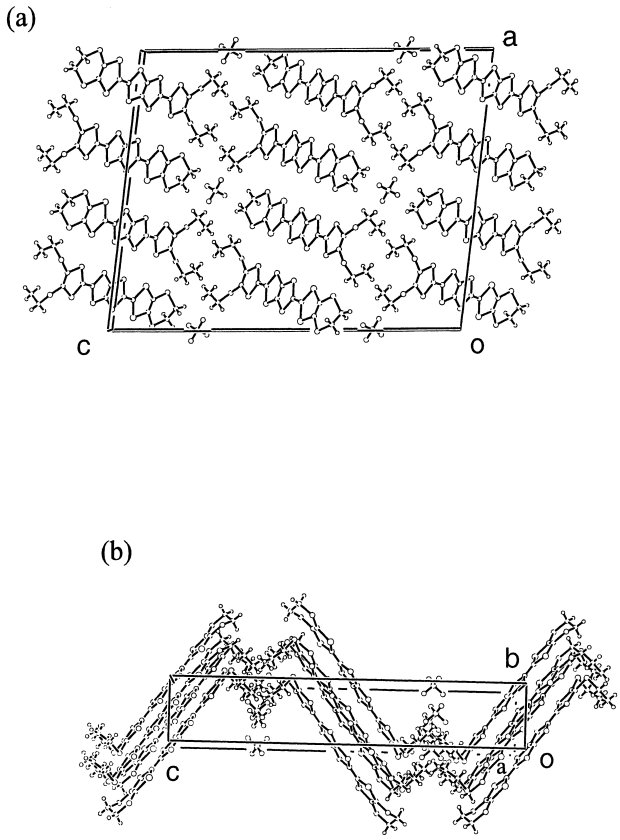


Fig. 2. Crystal structure of $(C_2TET\text{-}TS\text{-}TTP)_2ClO_4$, (a) projected along the b axis and (b) projected along the molecular short axis.

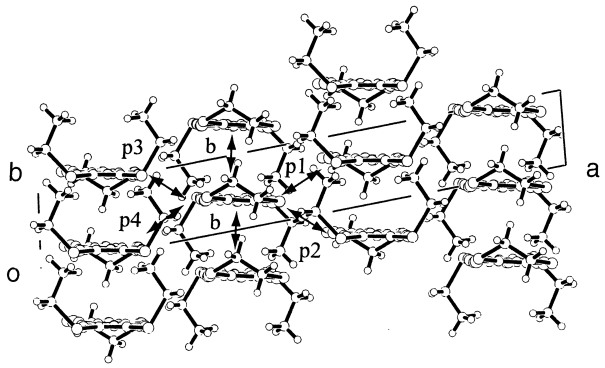


Fig. 3. Donor arrangement of $(C_2TET\text{-}TS\text{-}TTP)_2ClO_4$. The overlap integrals are $b = -15.1$, p1 = 5.0, p2 = 0.62, p3 = −0.32, and p4 = $5.2\times10^{-3}$.

As shown in Fig. 2(a), the donors in the neighboring chains are arranged in a head-to-tail manner.

The overlap integrals calculated from the overlap of HOMO are $b = -15.1$, p1 = 5.0, p2 = 0.62, p3 = −0.32, and p4 = $5.2\times10^{-3}$ (Fig. 3). The interstack interactions are about one third of the intrastack interaction. Therefore the interchain interaction is reasonably strong. The values of interchain transfer integrals p2 and p3 are particularly small in comparison with the S compound. This is because the expansion of the lattice occurs principally in the interchain direction. A tight-

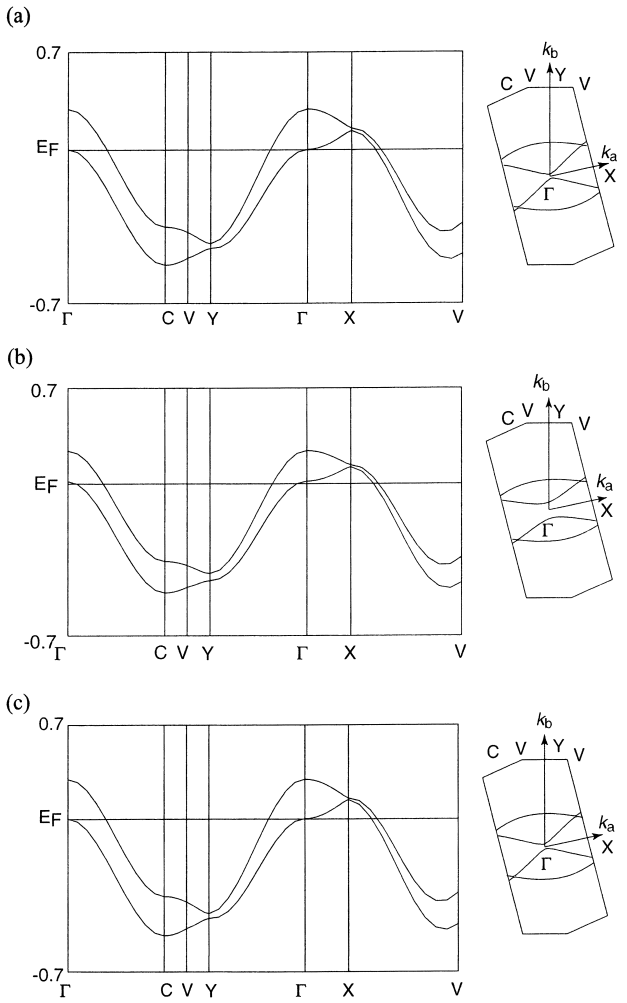


Fig. 4. Energy band structure and Fermi surface of the (a) $ClO_4^-$, (b) $BF_4^-$, and (c) $PF_6^-$ salts of $C_2$TET-TS-TTP.

binding energy band and Fermi surface are calculated on the basis of the extended Hückel method (Fig. 4).[10] Owing to the uniform donor stacks, the lattice constant $b$ along the stacking axis is very short, and the reciprocal lattice is elongated in the $k_b$ direction. This is one of the reasons that the Fermi surface is open perpendicularly to the $b$ axis. The Fermi surface is, however, considerably corrugated on account of the significant interchain interactions. It is difficult to decide whether the Fermi surface is connected near the $\Gamma$ point to result in a closed part or not, because the present system seems to be located near the boundary. However, since our parameters tend to overestimate interchain interactions in comparison with the intrachain interactions,[11] the absence of the closed part is likely.

In addition to this, X-ray single crystal structure analysis was carried out for another $C_2$TET-TS-TTP salt with a tetrahedral anion, $(C_2$TET-TS-TTP$)_2BF_4$. This salt is isostructural to $(C_2$TET-TS-TTP$)_2ClO_4$ (Table 2). The interplanar distance in a stack is 3.52 Å and the slip along the donor long axis is 4.76 Å. The overlap integrals calculated from the overlap of HOMO are $b = -14.6$, p1 = 3.7, p2 = 0.55, p3 = −0.68, and p4 = $4.4\times10^{-3}$. The Fermi surface is again open, as was that of $(C_2$TET-TS-TTP$)_2ClO_4$ (Fig. 4).

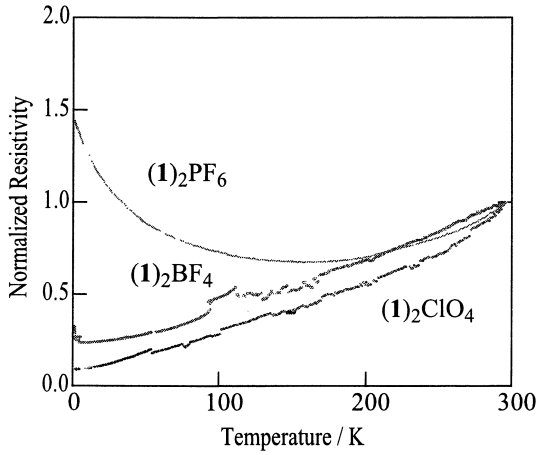


Fig. 5. Temperature dependence of the resistivities of the $ClO_4^-$, $BF_4^-$, and $PF_6-$ salts of $C_2$TET-TS-TTP.

A salt with an octahedral anion, $(C_2$TET-TS-TTP$)_2PF_6$ is also isostructural to the other $C_2$TET-TS-TTP salts with tetrahedral counter anions. Its increase of the lattice constants is, however, largest among the three salts (Table 2). The interplane distance in a stack is 3.51 Å, and the slip distance along the donor long axis is 4.79 Å. The overlap integrals calculated from the overlap of HOMO are $b = -15.4$, p1 = 5.0, p2 = 0.43, p3 = −0.39, and p4 = $5.4\times10^{-3}$. The tight-binding energy band structure and Fermi surface (Fig. 4) are similar to those of the other salts.

**Transport Properties.** $C_2$TET-TS-TTP salts with various anions were obtained as single crystals (Table 2). Among them, the cation radical salts with $ClO_4^-$, $BF_4^-$, and $PF_6^-$ are metallic down to low temperatures, although the salts with $I_3^-$ and $[Au(CN)_2]^-$ display semiconducting behavior.

Electrical resistivity values of $(C_2$TET-TS-TTP$)_2ClO_4$ and $(C_2$TET-TS-TTP$)_2BF_4$ are shown in Fig. 5. These salts show room-temperature conductivity of 55 S cm$^{-1}$ and 15 S cm$^{-1}$, respectively (cf. 900 S cm$^{-1}$ and 2500 S cm$^{-1}$ for the corresponding $C_2$TET-TTP salt).[4] The resistivity for $(C_2$TET-TS-TTP$)_2ClO_4$ decreases down to around 10 K, below which it is almost constant. The resistivity of $(C_2$TET-TS-TTP$)_2BF_4$ is metallic down to about 4.5 K, and slightly increases below this temperature.

The resistivity behavior of $(C_2$TET-TS-TTP$)_2PF_6$ is different from the other salts with tetrahedral anions (Fig. 5). This salt shows room-temperature conductivity of 34 S cm$^{-1}$, and exhibits a resistivity minimum around 150 K, below which the resistivity increases gradually to 1.5 K.

For the $I_3$ salt, the temperature dependence of resistivity is semiconducting, with a low room-temperature conductivity of $2.3\times10^{-4}$ S cm$^{-1}$ and activation energy of 0.086 eV. This may be related to the 1:1 composition expected from EDS. For the salt of $[Au(CN)_2]^-$, the resistivity is semiconducting with a room-temperature conductivity of 9.2 S cm$^{-1}$ and activation energy of 0.025 eV. The chemical analysis shows the $C_2$TET-TS-TTP:$[Au(CN)_2]$ composition to be 2:1. This may lead to its relatively high conductivity.

It is difficult to explain why the room-temperature conductivities of the $C_2$TET-TS-TTP salts are lower than those of the $C_2$TET-TTP salts. The crystal quality of the $C_2$TET-TS-TTP

salts seems to be as good as those of the $C_2$TET-TTP salts. It has been also observed in DTEDT that the selenium exchange of only one terminal 1,3-dithiole ring tends to reduce the conductivity.[12] This has been interpreted by the following reasoning; because the HOMO is mainly located on the central tetrathiapentalene moiety, the introduction of selenium atoms into only the outer 1,3-ditiole may weaken the intermolecular interactions.

## Conclusion

In conclusion, a newly prepared organic donor, $C_2$TET-TS-TTP, has yielded several cation radical salts by the electrochemical oxidation method. The $ClO_4^-$, $BF_4^-$, and $PF_6^-$ salts are metallic down to low temperatures. The three salts have the same uniform $\beta$-structures as that of $(C_2TET\text{-}TTP)_2ClO_4$.

For the sulfur donor, $C_2$TET-TTP, crystal structure has been known only for the $ClO_4^-$ salt. The $BF_4^-$ salt is probably isostructural. The present work proves that, for $C_2$TET-TS-TTP, not only the $ClO_4^-$ and the $BF_4^-$ salts, but also the $PF_6^-$ salt are isostructural. The $PF_6$ anion is a little larger than the tetrahedral anions, but can be incorporated within the $b = 5.9$ Å intervals. In contrast, the linear anions like $I_3^-$ and $[Au(CN)_2]^-$ are too long to be included parallel to the stacking direction. This seems to be associated with the semiconducting properties of these salts.

## Experimental

**Compound 3.** 2,3-Bis(2-cyanoethylthio)-6,7-bis(ethylthio)-TTF (**2**)[4] (670 mg, 1.35 mmol) was treated with excess cesium hydroxide monohydrate (100 mg, 10.8 mmol) in acetone, and the reaction mixture was stirred for 30 min under argon atmosphere. The reaction mixture was treated with zinc chloride (180 mg, 1.30 mmol) dissolved in methanol and stirred for 10 minutes, followed by treatment with tetrabutylammonium bromide (490 mg, 1.35 mmol) in methanol. After the reaction mixture was dried up in vacuo, the residue was suspended in dry THF, and then a large excess of acetic acid was added at −70 °C. The reaction mixture was allowed to warm up slowly to −25 °C, and an excess of 1,1′-thiocarbonyldiimidazole (240 mg, 1.35 mmol) was added. The mixture was allowed to warm up to room temperature overnight and the resulting precipitate was filtered and washed with small portions of methanol and hexane, and then dried in vacuo. Compound **3** (180 mg, 0.43 mmol) was obtained as red crystals in 53% yield.

mp 176 °C (dec.); IR (KBr) 2958, 2919, 1634, 1449, 1384, 1260, 1058, 963, 883, 763 $cm^{-1}$; $^1H$ NMR ($CDCl_3$) $\delta$ 1.32 (t, 6H, $J = 7.5$ Hz), 2.86 (q, 4H, $J = 7.5$ Hz); MS $m/z$ 430 ($M^+$).

**$C_2$TET-TS-TTP.** Compound **4** (180 mg, 0.4 mmol)[7] and **3** (320 mg, 0.8 mmol) in toluene (10 mL) were refluxed with a large excess of trimethyl phosphite (10 mL) under argon atmosphere for 2 hours. The mixture was cooled to room temperature and the resulting precipitate was filtered and washed with small portions of methanol and hexane. The solid was purified by column chromatography (silica gel/$CS_2$) to afford **1** (48 mg, 0.068 mmol) as a orange solid in 17% yield.

mp 218 °C (dec.); $^1H$ NMR ($CDCl_3$) $\delta$ 1.30 (t, 6H, $J = 7.4$ Hz), 2.84 (q, 4H, $J = 7.4$ Hz), 3.31 (s, 4H); MS $m/z$ 684 ($M^+$).

**Structure Determination.** The crystal structures of $(C_2TET\text{-}TS\text{-}TTP)_2ClO_4$, $(C_2TET\text{-}TS\text{-}TTP)_2BF_4$, and $(C_2TET\text{-}TS\text{-}TTP)_2PF_6$ were determined from single crystal X-ray diffraction; the crystallographic data are listed in Table 3. Intensity data were measured by the ω scan technique on a Rigaku automated four-circle diffractometer AFC-7R with graphite monochromatized Mo $K\alpha$ radiation ($2\theta < 60°$). The structures were solved by the direct method (SIR97 for the three compounds).[13,14] The structures were refined by the full-matrix least squares procedure by applying anisotropic temperature factors for all non-hydrogen atoms. Crystallographic data are deposited as Document No. 74026 at the Office of the Editor of Bull. Chem. Soc. Jpn.

**Electronic Band Structure.** The overlap integrals of the HOMO of $C_2$TET-TS-TTP were estimated on the basis of the extended Hückel method by substituting sulfur atomic orbitals for selenium.[10] The electronic band structures were calculated under the tight-binding approximation.

**Transport Properties.** Electric resistivity was measured for single crystals by the four-probe method using a low-frequency ac current (usually 10 μA). Electrical contacts to the crystals were made with 15 μm gold wire and gold paint. The crystals were held in a cryostat, and the temperature was monitored by a Cu–Constantan thermocouple and a carbon resistor sensor for above and below about 50 K, respectively. All measurements of transport properties are performed along the donor columns.

This work was partly supported by a Grant-in-aid for Science Research on Priority Areas (B) of Molecular Conductors and Magnets (No. 11224203) from the Ministry of Education, Science, Sports and Culture.

## References

1 Y. Misaki, H. Nishikawa, T. Yamabe, T. Mori, H. Inokuchi, H. Mori, and S. Tanaka, *Chem. Lett.*, **1992**, 2321.

2 T. Mori, T. Kawamoto, Y. Misaki, K. Kawakami, H. Fujiwara, T. Yamabe, H. Mori, and S. Tanaka, *Mol. Cryst. Liq. Cryst.*, **284**, 271 (1996), and references therein.

3 T. Mori, H. Inokuchi, Y. Misaki, H. Nishikawa, T. Yamabe, H. Mori, and S. Tanaka, *Chem. Lett.*, **1993**, 733; Y. Misaki, H. Nishikawa, T. Yamabe, T. Mori, H. Inokuchi, H. Mori, and S. Tanaka, *Chem. Lett.*, **1993**, 729.

4 S. Kimura, H. Kurai, T. Mori, H. Mori, and S. Tanaka, *Bull. Chem. Soc. Jpn.*, **74**, 59 (2001).

5 Y. Misaki, T. Kochi, T. Yamabe, and T. Mori, *Adv. Mater.*, **1998**, 588.

6 K. B. Simonsen, Niels Svenstrup, J. Lau, O. Simonsen, P. Mork, G. J. Kristensen, and J. Becher, *Synthesis*, **1996**, 407; M. Aragaki, T. Mori, Y. Misaki, K. Tanaka, and T. Yamabe, *Synth. Met.*, **102**, 1602 (1999).

7 R. Kato, H. Kobayashi, and A. Kobayashi, *Synth. Met.*, **41–43**, 2093 (1991).

8 A. Kobayashi, T. Udagawa, H. Tomita, T. Naito, and H. Kobayashi, *Chem. Lett.*, **1993**, 2179; H. Kobayashi, H. Tomita, T. Naito, A. Kobayashi, F. Sakai, T. Watanabe, and P. Cassoux, *J. Am. Chem. Soc.*, **118**, 368 (1996).

9 M. Kurmoo, M. Allan, R. H. Friend, D. Chasseau, G. Bravic, and P. Day, *Synth. Metals*, **42**, 2127 (1991); T. Mallah, C. Hollis, S. Bott, M. Kurmoo, P. Day, M. Allan, and R. H. Friend, *J. Chem. Soc., Dalton Trans.*, **1990**, 859.

10 T. Mori, *Bull. Chem. Soc. Jpn.*, **71**, 2509 (1998).

11 J. Ouyang, K. Yakushi, Y. Misaki, and K. Tanaka, *J. Phys. Soc. Jpn.*, **67**, 3191 (1998).

12 H. Fujiwara, Y. Misaki, T. Yamabe, T. Mori, H. Mori, and

S. Tanaka, *J. Mater. Chem.*, **10**, 1565 (2000).

13 G. M. Sheldrick, C. Kruger, R. Goddard, "Crystallographic Computing 3," ed by G. M. Sheldrick, Oxford University Press (1985), pp. 175–189.

14 A. Altomare, M. Cascrano, C. Giacovazzo, and A. Guagiliardi, *J. Appl. Cryst.*, **26**, 343 (1993).